

# Coulomb interaction rules timescales in potassium ion channel tunneling

N. De March, S. D. Prado and L. G. Brunnet

Instituto de Física, Universidade Federal do Rio Grande do Sul (UFRGS)

CP: 15051 Porto Alegre, RS, Brazil

E-mail: `nicole.march@ufrgs.br`

February 2018

**Abstract.** Assuming that the selectivity filter of KcsA potassium ion channel may exhibit quantum coherence, we extend a previous model by Vaziri & Plenio [1] to take into account Coulomb repulsion between potassium ions. We show that typical ion transit timescales are determined by this interaction, which imposes optimal input/output parameter ranges. Also, as observed in other examples of quantum tunneling in biological systems, addition of moderate noise helps coherent ion transport.

PACS numbers: 00.00, 20.00, 42.10

*Keywords:* quantum transport, quantum biology, ion channel, Coulomb repulsion 2

Submitted to: *J. Phys.: Condens. Matter*

## 1. Introduction

Ion channels are macromolecular pores-forming proteins in cell membranes that control the ion transport throughout the cell due solely to a concentration gradient. They have filters that select a specific ion, catalyze its dehydration, transfer and rehydrate it very efficiently. The so-called selectivity filter (SF) is part of a few angstrom wide protein that forms a tunnel inside the ion channel [2]. Potassium channels are the most studied types of ion channels since they are responsible for both establishing the resting potential in most cells and the asymptotic shape of the action potential in excitable cells.

The first crystallized potassium ion-channel KcsA of the bacteria (*Streptomyces lividians*) [3] has provided a better understanding on the SF structure. The KcsA filter is about 1.2 nm long with a diameter of 0.3 nm. It is believed that due to this narrowness and the fact that the incoming ions are without their hydration shell, the oxygen atoms of the carbonyl groups coordinate the ions motion into a single file fashion (Fig. 1). This is the fundamental structure under the four existing binding sites forming the ion path. While ion-channels structure may differ from bacterial to eukaryotic cells, the KcsA type remains relevant given that the SF structure is preserved across species. One of the most remarkable feature is the high current of  $10^8$  ions per second [4] which is comparable to the near free water diffusion speed [5].

Conflicting classical models have been proposed to explain the KcsA high throughput rate. They are mainly based on two mechanisms: cotranslocations of ions with water and knock-on. Ion translocation in KcsA is constructed considering states that alternate potassium ions e water molecules inside the filter. The main argument for cotranslocation relies on the large electrostatic repulsion between ions in adjacent sites, making it energetically unfavorable for two ions to occupy neighboring sites [6, 7]. So, although it would be possible to have ions side by side, given their size, it is assumed that two ions are typically separated by a single water molecule. The water being then responsible for the shielded Coulomb repulsion [6]. Besides that, the knock-on mechanism assumes that an incoming third ion interacts with the two ions inside the filter pushing them towards the flux direction driving the ion flow [8, 9]. In opposition, computational simulations [10, 11] have not only shown the possibility of configurations where water is not strictly transported between ions in a single file fashion but ions in adjacent sites were also possible. In other simulations were also assumed the stability of potassium ions close to each other and used the Coulomb repulsion as the main ingredient to drive the process efficiency [12, 13].

Inspired by the recent success in Quantum Biology [14, 15, 16, 17, 18, 19], a quantum model for the KcsA selectivity filter was proposed by Vaziri & Plenio [1]. They argue that given the ion-channel dimensions and the ion de Broglie wavelength associated with its thermal energy, the underlying dynamics for transport and selectivity might not be entirely classical. Within these assumptions, they propose a simplified model where a single particle can undergoes quantum tunneling to show that quantum coherence can give rise to significant effects. Even more interesting, they discuss a patch

clamp experiment where their hypothesis could be testified. Here, we improve their quantum model. Starting from the same hypothesis, we explore one further aspect that is Coulomb interaction in a two particle model. This is rather important, as highlighted above in the classical description of the phenomenon.

The paper is organized as follows. In Section 2, we estimate characteristic timescales for transport of repelling ions via perturbation theory and we build a two-particle model with Coulomb repulsion coupled to the environment via Lindblad operators. In Section 3 we show numerical results for ion transport, concluding that Coulomb repulsion dictates timescales and imposes bounds to the free parameters of our model. We add noise via dephasing and incoherent thermal hopping that reduces the system coherence time. We also observe that in a given range noise improves ion transport. This section is followed by the Conclusions.

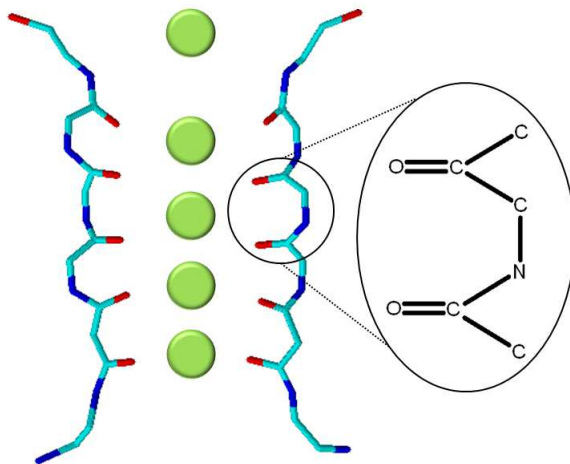


Figure 1: KcsA selectivity filter with four axial binding sites formed by peptide units H-N-C=O which carbonyl oxygen atoms C=O point toward the pore trapping a potassium ion or a water molecule.

## 2. Model & Methods

The KcsA selectivity filter consists in four binding sites for the ion. The axial separation between these potential minima is about 0.24 nm and, based on detailed molecular dynamics simulation [20], the potential barrier height varies between  $\sim 1.7 - 8.0 \ k_B T$  depending on both the protein thermal vibrations and the ion position in the channel. As propose in [1], we assume that a coherent process is behind the ion transmission, and we estimate the rates underlying the dynamics, mostly based on the available data for the current values.

First, each ion crossing the channel finds a sequence of potential barriers formed by carbonyl groups it may traverse by quantum tunneling. Approaching the potassium total energy by its thermal energy,  $E = k_B T/2 \approx 1.28 \times 10^{-2} \text{ eV}$ , and supposing a

rectangular potential barrier for simplicity, we can estimate a tunneling probability,  $p_{tun} \sim e^{-\Delta\sqrt{2m\Delta E/\hbar^2}}$ , with  $\Delta E$  the difference between the barrier energy  $1.7k_B T$  (the most favorable case) and the ion thermal energy. The barrier width,  $\Delta$ , is more difficult to estimate, but it certainly is smaller than the site distance, 0.24 nm. Due to the exponential character of the transmission as function of the barrier width, small variations  $\Delta$  imply large probability variations. Also, depending on the energy associated to the minimum of well potential between two consecutive barriers, the ion kinetic energy,  $K$ , can vary from  $\sim k_B T/2$  to  $\sim 1.7k_B T$  [13]. Approaching the ion frequency  $\nu = K/\hbar$  inside the well, we may find that the tunneling rate  $t_r \sim \nu p_{tun}$  may be given in the range  $t_r \sim 10^{11} - 10^{13} \text{ s}^{-1}$ .

From the experimental side, it is suggested in [1] an experimental setup where an ionic current of  $\sim 1 \text{ pA}$  could be possibly measured. But also, values of the order of  $\sim 10 \text{ pA}$  are found in classical molecular simulations [13]. So we have assumed the ionic current in the range from 1 pA to 10 pA and from that we estimate the rate of ions flowing through the channel of the order of  $\sim 10^7 - 10^8 \text{ s}^{-1}$ .

In this work, we deal with a two-particle model where coherent tunneling and Coulomb repulsion play a central role in ion transmission. We start investigating the relation between hopping rate in adjacent sites,  $c$ , and Coulomb repulsion  $U$ , using a second-order perturbation theory [21]. Assuming  $\hbar c \ll U$  yields an effective hopping  $c_{eff} \approx \hbar c^2/U$ , which is the effective tunneling rate between adjacent sites.  $c_{eff}$  imposes different system timescales as it will be shown later on. We associate the above measured ionic current to a maximum effective hopping rate, that is,  $c_{eff} \sim 10^7 - 10^8 \text{ s}^{-1}$  considering ions dehydrated of their water shielding,

$$U = \frac{ke^2}{a} \approx 5.14 \text{ eV}, \quad (1)$$

where  $a \sim 0.24 \text{ nm}$  is the distance between neighboring sites,  $k$  is the Coulomb's constant and  $e$  is the electron charge. The estimated effective hopping is then,

$$\frac{\hbar c^2}{5.14 \text{ eV}} \sim 10^7 - 10^8 \text{ s}^{-1}, \quad (2)$$

what yields a hopping rate close to the estimated tunneling rate

$$c \sim t_r \sim 10^{11} - 10^{13} \text{ s}^{-1} \quad (3)$$

So, the relation between Coulomb and hopping terms is  $U/\hbar c \sim 10^3 - 10^5$ .

The ion energy states inside the well may couple to vibrating energies of the carbonyl groups giving rise to dephasing and coherence loss [1]. Here we consider the simplest possible model for two particles with a simple site independent dephasing to account for these carbonyl oscillations through a specific non-unitary term in the dynamics. Another thermal effect is the possible incoherent scattering caused by oscillations in the potential barrier height, which is treated as another noise term as it is shown below.

### 2.1. The quantum model

Improving the model [1] we consider a two particle system with Coulomb interaction in a one-dimensional lattice. We use a tight-binding Hamiltonian for the linear chain of potential barriers, each ion in the SF may cross it through coherent tunneling. The Hamiltonian that describes the unitary evolution is given by

$$H = -\hbar \sum_{j=1}^4 c \left( \sigma_j^\dagger \sigma_{j+1} + \sigma_{j+1}^\dagger \sigma_j \right) + V, \quad (4)$$

where  $\hbar$  is the Planck's constant divided by  $2\pi$ ,  $j$  is the site label,  $c$  is the hopping rate taken equal for all sites.  $\sigma_j^\dagger$  ( $\sigma_j$ ) is the creation (annihilation) operator for fermions in  $j$ th-site, avoiding two ions in the same well. The potential energy  $V$  due to the Coulomb repulsion is given by

$$V = \frac{1}{2} \sum_{j=1}^4 \sum_{j' \neq j=1}^4 \frac{U}{|j-j'|} \sigma_j^\dagger \sigma_j \sigma_{j'}^\dagger \sigma_{j'}. \quad (5)$$

To simulate the SF exchange of ions with the environment, extra sites are linked on each side of the chain [22, 23]. A site labeled site-0 acting as an external *source* of particles, is connected with site-1, the first internal SF site. The second extra site, site-6, is connect with the SF site-5 and acts as a *drain*. Its role is to remove ions from the channel. It is worth emphasizing that source and drain here are very poorly compared to typical thermal baths, since they only act supplying (source) and leaking (drain) particles to/from the channel. They do introduce decoherence into the system as we discuss later on, but many of the most important interactions that rule the interaction of a system coupled to thermal baths are indeed not considered in our model.

This approach is formalized by using the following Lindblad operators [24]:

$$\mathcal{L}_s(\rho) = \Gamma_s \left( - \left\{ \sigma_0^\dagger \sigma_1 \sigma_1^\dagger \sigma_0, \rho \right\} + 2 \sigma_1^\dagger \sigma_0 \rho \sigma_0^\dagger \sigma_1 \right), \quad (6)$$

where  $s$  stands for source,  $\Gamma_s$  denotes source supplying rate and  $\rho = \rho(t)$  is the density matrix (DM). Similarly to Eq.(6), the correspondent Lindblad operator for the drain is given by

$$\mathcal{L}_d(\rho) = \Gamma_d \left( - \left\{ \sigma_5^\dagger \sigma_6 \sigma_6^\dagger \sigma_5, \rho \right\} + 2 \sigma_6^\dagger \sigma_5 \rho \sigma_5^\dagger \sigma_6 \right), \quad (7)$$

where  $d$  stands for drain and  $\Gamma_d$  denotes the leaking rate of the drain.

The drain is populated as the ions are transferred along the channel. One can then investigate the rate at which the drain is populated in order to study the channel transport efficiency. We do not assume Coulomb repulsion for the ions while they are in the source or in the drain, as one can assume them dressing a hydration shell. Another assumption, included in the Lindblad formalism, is a Markovian process for drain and source. Memory effects may be important if ion dynamics of drain and source fluctuate

due to external environment conditions. However, here we concentrate in exploring the role of Coulomb interaction among the ions inside the channel and neglect these external fluctuations.

In this context it is natural to use a fermion number occupation basis for the ion-channel sites (1 to 5), avoiding two particles in the same site. On the other hand, source and drain are treated in a boson occupation basis, since it is irrelevant to the dynamics inside the channel. This results in a density matrix composed by 23 squared terms.

Still following [1], we model the thermal vibrations of the carbonyl groups adding a noise term that randomizes the local phase excitations at a rate  $\gamma_{deph}$ . Thus, we will assume a model where noise is local and use the following Lindblad superoperator.

$$\mathcal{L}_{deph}(\rho) = \sum_{j=1}^5 \gamma_{deph} \left( -\left\{ \sigma_j^\dagger \sigma_j, \rho \right\} + 2\sigma_j^\dagger \sigma_j \rho \sigma_j^\dagger \sigma_j \right), \quad (8)$$

This dephasing produces an exponential decay of the DM terms with the rate  $\gamma_{deph}$  [25]. Besides the random phase, we also consider another term that takes into account particles jumping incoherently due to thermal excitations. This incoherent scattering also produces an exponential decay of the elements of DM implying in loss of coherence. It is given by

$$\begin{aligned} \mathcal{L}_{th}(\rho) = & \sum_{j=1}^4 \Gamma_{th} \left[ 2\sigma_{j+1}^\dagger \sigma_j \rho \sigma_j^\dagger \sigma_{j+1} - \left\{ \sigma_j^\dagger \sigma_{j+1} \sigma_{j+1}^\dagger \sigma_j, \rho \right\} \right] \\ & + \sum_{j=1}^4 \Gamma_{th} \left[ 2\sigma_{j+1} \sigma_j^\dagger \rho \sigma_j \sigma_{j+1}^\dagger - \left\{ \sigma_j \sigma_{j+1}^\dagger \sigma_{j+1} \sigma_j^\dagger, \rho \right\} \right], \end{aligned} \quad (9)$$

where  $\Gamma_{th}$  is the thermal rate.

Thus, the evolution of the system is obtained by the integration of the following Lindblad master equation [24, 26]

$$\frac{d}{dt}\rho(t) = -\frac{i}{\hbar} [H, \rho(t)] + \mathcal{L}_s(\rho) + \mathcal{L}_d(\rho) + \mathcal{L}_{deph}(\rho) + \mathcal{L}_{th}(\rho). \quad (10)$$

which defines a set of coupled linear ordinary differential equations.

### 3. Numerical results

The numerical results presented here are for adimensionalized parameters. They are rescaled by the effective hopping  $c_{eff} \approx \hbar c^2/U$  discussed in 2. So, the adimensional time is given by  $\tau = t c_{eff}$  and a adimensionalized rate  $(\cdot)$  is rescaled as  $(\tilde{\cdot}) = (\cdot)/c_{eff}$ . From Equation 3 we assume  $c$  in the range  $[10^{11} - 10^{13}]s^{-1}$ , which combined with Equation 1 results  $\mathcal{U} = U/\hbar c$  in the range  $[10^3 - 10^5]$ . We set  $\hbar = c = 1$ , so that  $\mathcal{U} = U$  and results are shown for the adimensionalized  $U$ , for convenience. Also, the initial condition is always two particles at site-0, the source.

As discussed above in section 2, different  $U$  values imply different timescales for the system. In Fig. (2) it is shown the site-5 population for different  $U$  values as function of reduced time. The same curves are shown in the inset but without time rescaling. Note that, as expected, the larger the Coulomb repulsion the slower the dynamics. Recall that site-5 population determines the drain occupation, since the Lindblad operator connects them through Equation (7).

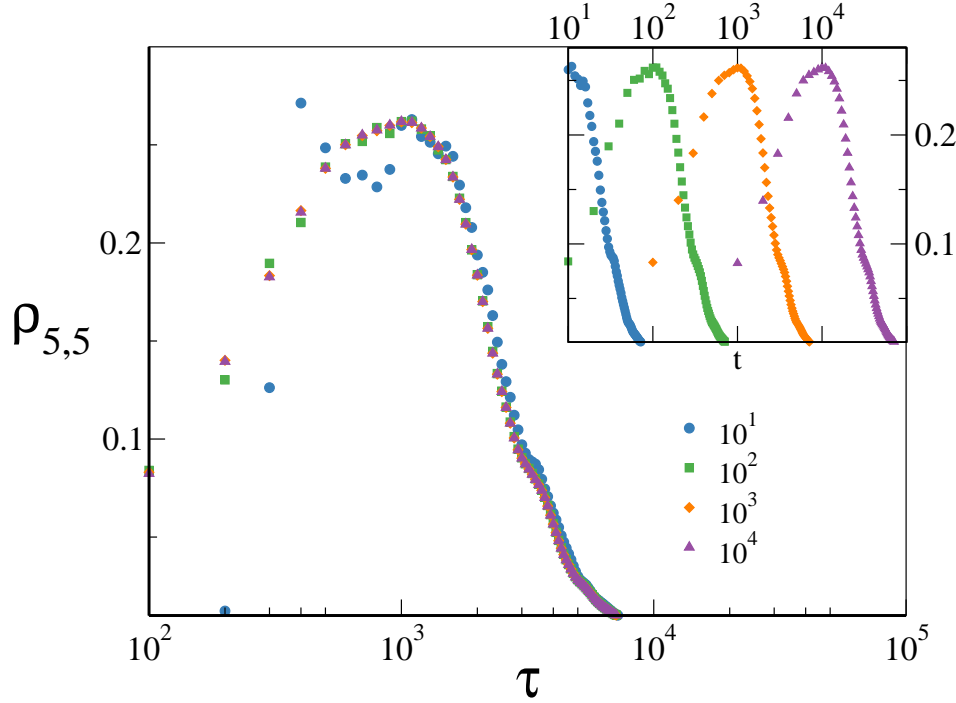


Figure 2: (Color online) Site-5 population versus reduced time (logarithmic scale in  $\tau$ -axis) for different values of  $U$  for  $\tilde{\Gamma}_s = \tilde{\Gamma}_d = 1$  and  $(\tilde{\gamma}_{deph} = \tilde{\Gamma}_{th} = 0)$ . Raw data are shown in the inset with the same convention. The curves matching shows the time rescaling with Coulomb repulsion.

Given that the same dynamics is obtained if we correctly rescale time using Coulomb repulsion, we may set a value for  $U$ . So, for the remaining results in this paper we set  $U = 10^3$ , which is the lower border of the estimated interval for  $U$ . We then have investigated different scenarios generated by constraints imposed by the external rates. In particular, we are interested in searching an optimal ion flow in the parameter space generated by these different rates.

Fig. 3(a) shows drain population,  $\rho_d = \rho_{6,6}$ , for different  $\tilde{\Gamma}_s$  values and  $\tilde{\Gamma}_d = 1$ . At short times ( $\tau \lesssim 1$ ) the drain is populated faster for  $\tilde{\Gamma}_s > 1$ . In the case  $\tilde{\Gamma}_s = 1$  there is a slower dynamics at short times but at longer times it grows faster and the drain is fulfilled at the same time than for  $\tilde{\Gamma}_s > 1$ . Fig. 3(b) shows the time derivative of the drain population. Note that this derivative oscillates. The high frequency oscillations that dominate short times are consequence of hopping and the low frequency of effective hopping, the later is more pronounced when the particle injection is faster than  $\tilde{\Gamma}_s > 1$ .

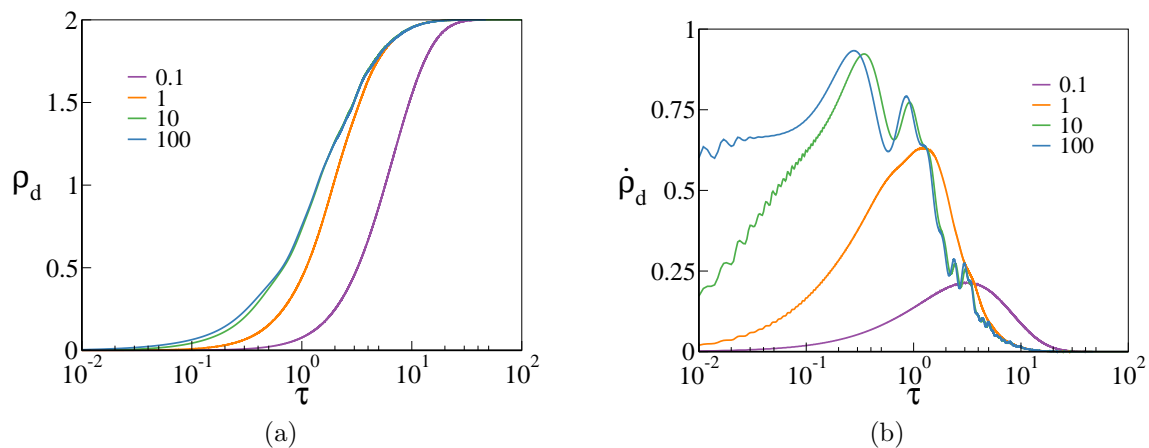


Figure 3: (Color online) (a) Drain population  $\rho_d$  and (b) its time derivative  $\dot{\rho}_d$  for the source rate  $\tilde{\Gamma}_s$  indicated. Drain rate  $\tilde{\Gamma}_d = 1$ .

Now we explore cases varying drain rates for a constant rate input. Fig. 4(a) illustrates the case. The drain is fully occupied faster when  $\tilde{\Gamma}_d = 1$  (inset in Fig. 4(a)). When the drain occupation is asymptotically close to two particles, the dynamics slows down for  $\tilde{\Gamma}_d > 1$ . Similarly to Fig. 3(b) we observe in Fig. 4(b) high frequency oscillations as a hopping consequence. In Fig. 4(b) the drain is occupied fast for larger values of  $\tilde{\Gamma}_d$  up to the time when site-5 occupation is maximum. After that time, larger values of  $\tilde{\Gamma}_d$  implies depletion of site-5 occupation (Fig. 5).

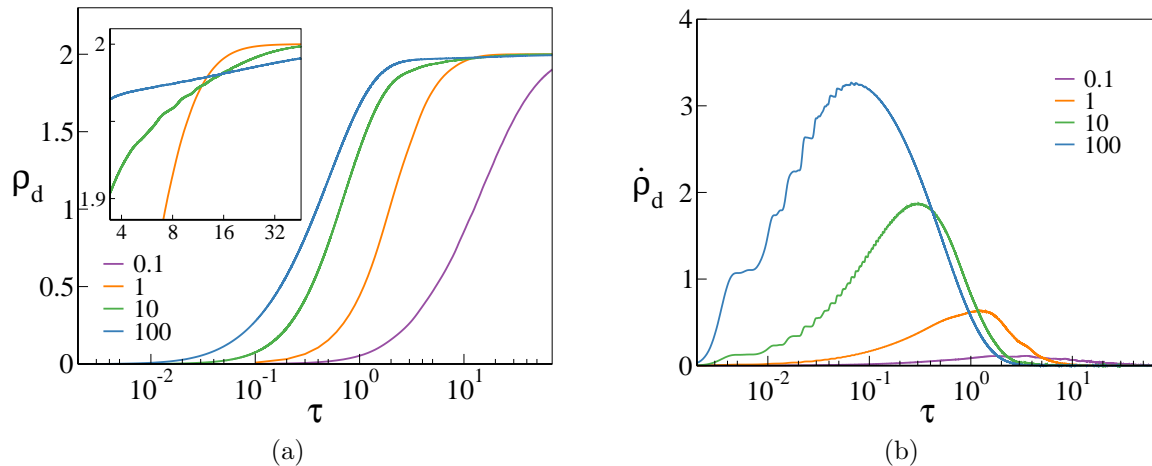


Figure 4: (Color online) (a) Drain population  $\rho_d$  and (b) its time derivative  $\dot{\rho}_d$  for the drain rate  $\tilde{\Gamma}_d$  indicated. Source rate  $\tilde{\Gamma}_s = 1$ .



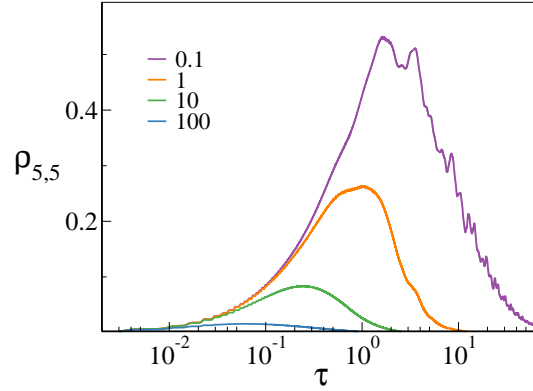


Figure 5: (Color online) Site 5-occupation versus time for indicated drain rates  $\tilde{\Gamma}_d$  and source rate  $\tilde{\Gamma}_s = 1$ .

#### 4. Noise-assisted Transport

The results presented in the last section for ion transport properties were for a system without any noise added. Now, it is expected that noise always ruin coherence. So, in what follows we analyse the impact of dephasing and thermal noises on the transport.

Coherence is investigated analyzing the off-diagonal terms of the channel reduced density matrix. For that we use the  $l_1$ -norm defined as [27]

$$C(\tau) = \sum_{i \neq j} |\rho_{ij}(\tau)|. \quad (11)$$

In our simulations the system is considered coherent for times up to  $\tau$  such that  $C(\tau) \gtrsim 10^{-2}$  that correspond to real times of order  $10^{-8}$ s in agreement with [1].

Fig. 6(a) shows  $C(\tau)$  at constant  $\tilde{\Gamma}_s = 1$  for different values of  $\tilde{\Gamma}_d$  (non-continuous lines,  $\tilde{\Gamma}_d$  values indicated in the figure). The channel population respective to each  $\tilde{\Gamma}_d$  case is shown by the solid lines. Clearly  $C(\tau)$  follows the same behavior of the of remaining occupation inside the channel. Also, as above in Fig. 4(a), drain is more quickly filled up when  $\tilde{\Gamma}_d = 1$ . In Figs. 6(b) and 6(c) triangles indicate 1.99 as particle occupation in the drain, or 0.01 still in the channel. This number was arbitrarily set but recall that it still satisfies the condition that the dynamics is coherent up to the time this drain occupation is fulfilled.

Fig. 6(b) shows the coherence  $C(\tau)$  when  $\tilde{\Gamma}_s = \tilde{\Gamma}_d = 1$  for different values of  $\tilde{\gamma}_{deph}$ . We observe that a dephasing noise in the order of the system characteristic timescale ( $\tilde{\gamma}_{deph} \lesssim 1$ ) favors drain filling. Note the occupation triangles indicating a faster drain filling for these cases.

Fig. 6(c) shows that thermal noise always reduces drain filling time. However coherence loss is more pronounced than with noise dephasing, at least for  $\tilde{\Gamma}_{th} > 1$ . The occupation triangle for  $\tilde{\Gamma}_{th} = 100$ , for example, happens for  $C(\tau) \sim 10^{-5}$ . So the system is not considered coherent any longer. On the other hand, for  $\tilde{\Gamma}_{th} \leq 1$  coherence is preserved and filling drain times are smaller than in the noiseless system.

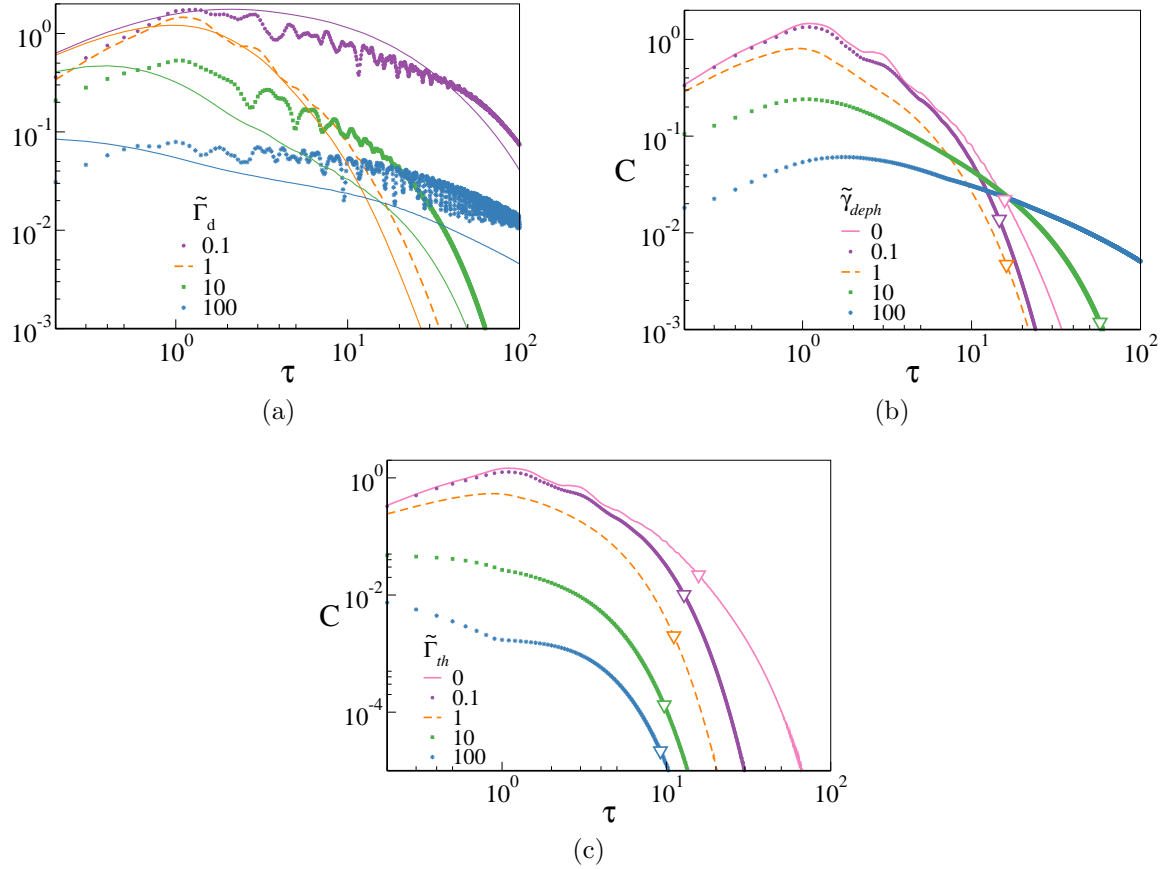


Figure 6: (Color online)(a) Coherence evolution (non-continuous lines) and occupation inside the channel (continuous lines) for different  $\tilde{\Gamma}_d$  values at constant  $\tilde{\Gamma}_s = 1$ . (b) Coherence evolution for different  $\tilde{\gamma}_{deph}$  values, drain occupation limit of 1.99 for  $\tilde{\gamma}_{deph} = 10$  is reached for  $\tau > 300$  (not shown). (c) different  $\tilde{\Gamma}_{th}$  at constant  $\tilde{\Gamma}_s = \tilde{\Gamma}_d = 1$ , down triangles indicate when  $\rho_d = 1.99$ .

## 5. Conclusions

Previous single particle models [1] suggest that tunneling rates in the order of  $10^8 s^{-1}$  may explain ion channel high efficiency transport. However such models ignore the presence of a large Coulomb interaction, which has been shown to display a relevant role in classical approaches [12, 13]. So, here we improve the model considering a two-particle system with Coulomb repulsion. This interaction is known to slow down the dynamics, particularly when the interaction is strong, which is the case here. Nevertheless, small changes in the estimated values for the potential barrier may alter hopping characteristic scales to ranges  $[10^{11} - 10^{13}] s^{-1}$ , around  $10^3$  times faster than previously estimated [1], resulting in an effective hopping term still compatible with expected values for the channel current, while keeping a coherent quantum system.

Our simulations show that ion transport is optimized if source input and drain output rates are compatible with the system characteristic time, as defined by the

relation  $c_{eff} = \hbar c^2/U$ . Besides the optimization, when the rates are adjusted any other Coulomb effect than different timescale is minimized. Considering larger rates, e.g.,  $\tilde{\Gamma}_s > 1$  or  $\tilde{\Gamma}_d > 1$ , results in lower ion currents and a larger dwell time for the ions inside the channel. This remaining charge oscillates with the system characteristic time, as indicates the current derivative.

In order to check the possibility of improving charge transport with noise, as in Ref. [1], we varied dephasing rate and thermal noise over four orders of magnitude. Simulations show that dephasing noise levels in the order of one or smaller enhance charge transport. Thermal noise increases ion transport independently of its intensity, however, in this case coherence is lost for values above one.

In fact, these operators also artificially impose input/output rates to emulate ion concentrations outside the channel. But the presence of Coulomb repulsion dictates a characteristic timescale for channel flow. So, if ion concentration is below some optimal value, we expect a high flux since the problem is reduced to a single particle one with a hopping one thousand times faster. On the other side, if ion concentration is above this optimal value, dynamics slows down and we observe oscillations in current derivatives. In any case we do not expect a linear relation between ion concentration and current.

## Acknowledgments

We thank the Brazilian agencies CAPES, CNPq, and FAPERGS for financial support. We also acknowledge the Computational Center of the Physics Institute of UFRGS for cluster computing hours.

## References

- [1] Vaziri A and Plenio M B 2010 *New Journal of Physics* **12** 085001
- [2] Roux B and Schulten K 2004 *Structure* **12** 1343–1351
- [3] Doyle D A, Cabral J M, Pfuetzner R A, Kuo A, Gulbis J M, Cohen S L, Chait B T and MacKinnon R 1998 *Science* **280** 69–77
- [4] Gouaux E and MacKinnon R 2005 *Science* **310** 1461–1465
- [5] Hille B *et al.* 2001 *Ion Channels of Excitable Membranes* vol 507 (Sinauer Sunderland, MA)
- [6] Morais-Cabral J H, Zhou Y and MacKinnon R 2001 *Nature* **414** 37–42
- [7] Zhou Y and MacKinnon R 2003 *Journal of Molecular Biology* **333** 965–975
- [8] Hodgkin A L and Keynes R 1955 *The Journal of Physiology* **128** 61–88
- [9] Berneche S and Roux B 2001 *Nature* **414** 73–77
- [10] Furini S and Domene C 2009 *Proceedings of the National Academy of Sciences* **106** 16074–16077
- [11] Fowler P W, Abad E, Beckstein O and Sansom M S 2013 *Journal of Chemical Theory and Computation* **9** 5176–5189

- [12] Bordin J R, Diehl A, Barbosa M C and Levin Y 2012 *Physical Review E* **85** 031914
- [13] Köpfer D A, Song C, Gruene T, Sheldrick G M, Zachariae U and de Groot B L 2014 *Science* **346** 352–355
- [14] Ball P 2011 *Nature News* **474** 272–274
- [15] Lloyd S 2011 Quantum coherence in biological systems *Journal of Physics: Conference Series* vol 302 (IOP Publishing) p 012037
- [16] Lambert N, Chen Y N, Cheng Y C, Li C M, Chen G Y and Nori F 2013 *Nature Physics* **9** 10
- [17] Buchleitner A, Burghardt I, Cheng Y C, Scholes G D, Schwarz U T, Weber-Bargioni A and Wellens T 2014 *New Journal of Physics* **16** 105021
- [18] Mohseni M, Omar Y, Engel G S and Plenio M B 2014 *Quantum effects in biology* (Cambridge University Press)
- [19] Salari V, Naeij H and Shafiee A 2017 *Scientific Reports* **7** 41625
- [20] Gwan J F and Baumgaertner A 2007 *The Journal of Chemical Physics* **127** 045103
- [21] Sakurai J J and Napolitano J J 2014 *Modern Quantum Mechanics* (Pearson Higher Ed)
- [22] Plenio M B and Huelga S F 2008 *New Journal of Physics* **10** 113019
- [23] Bassereh H, Salari V and Shahbazi F 2015 *Journal of Physics: Condensed Matter* **27** 275102
- [24] Breuer H P and Petruccione F 2002 *The Theory of Open Quantum Systems* (Oxford University Press on Demand)
- [25] Contreras-Pulido L, Bruderer M, Huelga S and Plenio M 2014 *New Journal of Physics* **16** 113061
- [26] Rivas A and Huelga S F 2012 *Open Quantum Systems* (Springer)
- [27] Baumgratz T, Cramer M and Plenio M 2014 *Physical Review Letters* **113** 140401